JOURNAL OF CATALYSIS 67, 90–102 (1981)

The Chemistry and Catalysis of the Water Gas Shift Reaction

1. The Kinetics over Supported Metal Catalysts

D. C. GRENOBLE[1] AND M. M. ESTADT

Corporate Research Laboratories, Exxon Research and Engineering Company, P.O. Box 45, Linden, New Jersey 07036

AND

D. F. OLLIS

Department of Chemistry and Chemical Engineering, University of California at Davis, Davis, California 95616

Received January 9, 1980; revised July 28, 1980

The water gas shift (WGS) reaction ($CO + H_2O \rightarrow CO_2 + H_2$) is catalyzed by many metals and metal oxides as well as recently reported homogeneous catalysts. In this present paper the kinetics of the WGS reaction as catalyzed by alumina-supported Group VIIB, VIII, and IB metals are examined. For several metals a strong effect of support on metal activity is observed. For example, the turnover number (rate per surface metal atom) of Pt supported on Al_2O_3 is an order of magnitude higher than the turnover number of Pt on SiO_2. The turnover numbers (at 300°C) of the various alumina-supported metals studied for WGS decrease in the order Cu, Re, Co, Ru, Ni, Pt, Os, Au, Fe, Pd, Rh, and Ir. For these metals the range of activity varies by more than three orders of magnitude. It is shown that a volcano-shaped correlation exists between the activities of these metals and their respective CO heats of adsorption. The partial pressure dependencies of the reactants on these metals are reported for the first time. Over most metals the CO order of reaction is near zero and the H_2O order of reaction is near $\frac{1}{2}$. A reaction sequence including formic acid as an intermediate is proposed in order to account for the apparent bifunctionality of the supported catalyst systems. This approach leads to a power rate law, $r = kP_{CO}{}^{X}P_{H_2O}{}^{(1-X)/2}$, an expression shown to be consistent with the experimental parameters obtained in these kinetic studies.

INTRODUCTION

The water gas shift (WGS) reaction, a reaction of considerable industrial importance, is the reaction of water and carbon monoxide to produce carbon dioxide and hydrogen:

$$CO + H_2O \rightarrow CO_2 + H_2. \quad (1)$$

The WGS process is most frequently used in conjunction with the production of hydrogen via the steam reforming of hydrocarbons:

$$C_nH_m + n\,H_2O \rightarrow n\,CO + (n + m/2)H_2, \quad (2)$$

$$CO + H_2O \leftrightarrows CO_2 + H_2, \quad (3)$$

$$CO + 3H_2 \leftrightarrows CH_4 + H_2O. \quad (4)$$

Reaction (2), under steam-reforming conditions (typically about 800°C), is considered irreversible and essentially complete. Normally reactions (3) and (4) at the exit of the steam-reforming reactor are nearly at equilibrium. The high temperature in the reformer favors H_2 production by shifting the equilibrium of reaction (4) far to the left. The effluent from the steam reformer is then passed to a series of WGS reactors which are operated at lower temperatures

[1] Present address: Exxon Chemical Co., P.O. Box 271, Florham Park, N.J. 07932. To whom correspondence should be mailed.

0021-9517/81/010090-13$02.00/0

in order to shift the equilibrium of reaction (3) to the right. At intermediate temperatures (400–500°C) the WGS catalyst is based on iron oxides. At still lower temperatures (150–200°C) the catalyst of choice is based on copper. A description of commercial catalysts can be found in Ref. (*1*).

The most important use of WGS technology is in the production of H_2 as described above. However, the WGS reaction can occur whenever CO and H_2O are present in a reacting mixture. For example, in the methanation reaction (reaction (4)), which is the simplest reaction of the complex Fischer–Tropsch syntheses, the water product can react with CO feed via the WGS reaction. The activity of the catalyst for WGS may thus control the selectivity to water or CO_2. Other areas where WGS may play an important role in the overall chemistry include hydrocarbon oxidation reactions and auto exhaust combustion catalysis.

Our interest in the WGS reaction grew out of previous studies of the toluene steam dealkylation (TSD) reaction (*2*, *3*):

(5)

Reaction (5) represents the simplest stoichiometry for describing the TSD reaction. However, the principal carbon oxide product is carbon dioxide and not carbon monoxide. The carbon dioxide is formed from the subsequent water gas shift of the carbon monoxide primary product. Thus the WGS reaction is fast relative to the TSD reaction. The catalysts selected for TSD are generally noble metals as they have the highest selectivities toward benzene formation (see Ref. (*2*). Because WGS and TSD are catalyzed by the same materials, it was of interest to compare the kinetics of these two reactions. Of particular interest was a comparison of the effect of support on both reactions. These support effects will be discussed in this paper. The second paper of this series will discuss in detail the comparison of the kinetics of WGS and TSD reactions. Although our primary interest has been the kinetics of the WGS reaction over Group VIII noble metals, the growing interest in Fischer–Tropsch chemistry prompted us to extend these studies to include the Group VIII iron triad as well as one Group VIIB metal (Re) and two Group IB metals (Cu and Au).

The WGS reaction is readily catalyzed by both metals and metal oxides. Recently, homogeneous catalysts have also been described (*4*). It has long been recognized that many Group VIII metals catalyze the steam-reforming reactions (*5*, *6*) as discussed above. Nevertheless there are only a few reports of studies which focus on the kinetics of the WGS reaction over Group VIII metals other than iron. Prichard and Hinshelwood (*7*) in 1925 studied the kinetics of the reverse WGS reaction, $CO_2 + H_2 \rightarrow CO + H_2O$, over platinum. More recently, Japanese workers (*8*, *9*) have investigated the kinetics of the WGS reaction over platinum. Shelef and Gandhi (*10*) have reported that the WGS reaction is catalyzed by Ru. Taylor *et al.* (*11*) have also shown that the WGS reaction occurs over Ru, Pt, and Pd catalysts. In this present work we have made a detailed study of both the kinetics and the specific activities of a number of supported metal catalysts for the WGS reaction, an aspect which has been lacking in previous investigations. These kinetic studies indicate bifunctional catalyst activity and lead to a power rate law expression generally consistent with the observed kinetic parameters for all the metals studied.

EXPERIMENTAL

The apparatus and techniques used for the kinetic studies and chemisorption studies were previously described in Ref. (*2*). In general the deactivation rate of the catalysts for WGS was not as great as that for the TSD reaction. Nevertheless, "bracketing" techniques described in Ref.

(*2*) were employed to assure the determination of unbiased kinetic parameters.

Prior to kinetic parameter measurements, all catalysts except Cu and Au were reduced in flowing H_2 at 500°C for 1 hr. The Cu and Au catalysts were reduced at 250°C for the same period. All rate constants discussed in this report were obtained at standard conditions of water and CO partial pressures of 31.4 and 24.3 kPa, respectively. Reaction temperatures were varied to maintain CO conversion of less than 5%, thus assuring reactor operation in a differential mode with negligible heat and mass transfer effects. The metal dispersions of all catalysts except the Cu, Au, Co, and Fe catalysts were previously determined with H_2 chemisorption (*2, 12*). The metal surface areas of the Cu/Al_2O_3 and Au/Al_2O_2 catalysts were determined by X-ray line broadening techniques, the Fe catalyst by CO chemisorption, and the Co catalyst by H_2 chemisorption.

The preparations of all catalysts except the Au, Cu, Fe, and Co catalysts were previously described (*2, 12*). These latter catalysts were prepared by incipient wetness techniques using aqueous solutions of the following salts: $AuCl_4 \cdot 3H_2O$, $Cu(NO_3) \cdot 3H_2O$, $Co(NO_3)_2 \cdot 6H_2O$, and $Fe(NO_3) \cdot 9H_2O$. The alumina support used was γ-Al_2O_3 (Engelhard Industries), the silica was Cab-O-Sil (Cabot Corp.), and the carbon was Carbolac (Cabot Corp.). The carbon monoxide used was ultrahigh purity (Matheson Gas).

RESULTS

The dispersion, or fraction exposed, values of all the catalysts studied are presented in Table 1. As appropriate for the catalysts, one chemisorbed hydrogen atom or CO molecule was assumed to represent one surface metal atom. The X-ray line broadening technique was less reliable than chemisorption methods, but was utilized because of the lack of strong H_2 and CO chemisorption on Cu and Au.

TABLE 1

Dispersions of Catalysts

Catalyst $\%M/Al_2O_3$	H_2 uptake (μ mole/g cat)	Fraction exposed
A. Alumina-supported metals		
1% Ru	10.2	0.21
1% Ru	47.7	0.98
1% Pd	13.2	0.28
2% Os	12.3	0.23
2% Ir	94.1	1.0
2% Pt	60.1	1.0
10% Fe	17.0[a]	0.01
5% Co	9.6	0.02
5% Ni	77.3	0.18
10% Re	23.1	0.08
10% Cu	[b]	0.03
5% Au	[b]	0.13
B. Other catalyst systems		
2% Pt/SiO_2	40.2	0.78
4% Pt/C	110.0	1.00
2% Rh/SiO_2	69.7	0.72

[a] CO chemisorption uptake.
[b] X-Ray line broadening technique used.

The kinetic parameters obtained for the WGS reaction over the Al_2O_3-supported metals are presented in Table 2. Two metals (Pt and Rh) were also studied on additional supports: their kinetic parameters are presented in Table 3. The activities listed in Tables 2 and 3 are turnover rates (rates per surface atom) for each catalyst at 300°C. When activities were not specifically measured at 300°C, the activities were calculated at 300°C using the Arrhenius expression $r = A \exp(-E_a/RT)$, where E_a is the apparent activation energy and A is the preexponential factor. These parameters are included in Tables 2 and 3. All activities except those for Cu and Pd were measured within 50° of 300°C, thereby minimizing extrapolation errors. At standard conditions of partial pressures and 300°C the relative turnover numbers of the alumina-supported metals are: Cu, 3800; Re, 120; Co, 77; Ru, 60; Ni, 32; Pt, 20; Os, 19; Au, 9; Fe, 5; Pd, 4; Rh, 3; Ir, 1.

The experimental orders of reaction with

TABLE 2

Kinetic Parameters of Alumina-Supported Metals for WGS Reaction

Catalyst %M/Al_2O_3	Temp[a]	X[b]	Y[c]	E[d]	A[e]	N[f,g]
1% Ru	290	−0.21 ± 0.08	0.66 ± 0.08	22.5 ± 0.6	7.38×10^7	0.1929
1% Rh	330	−0.10 ± 0.02	0.44 ± 0.08	23.0 ± 1.3	5.00×10^6	0.0086
1% Pd	380	0.14 ± 0.06	0.38 ± 0.07	19.1 ± 0.7	2.61×10^5	0.0135
2% OS	320	−0.27 ± 0.08	0.63 ± 0.02	23.6 ± 2.7	6.18×10^7	0.0615
2% Ir	350	0.03 ± 0.04	0.48 ± 0.06	20.6 ± 3.3	2.31×10^5	0.0032
2% Pt	270	−0.21 ± 0.03	0.75 ± 0.04	19.6 ± 1.3	1.91×10^6	0.0635
10% Fe	350	0.58 ± 0.12	0.04 ± 0.12	19.2 ± 1.3	3.18×10^5	0.0151
5% Co	250	−0.35 ± 0.12	0.67 ± 0.12	11.3 ± 3.6	5.05×10^3	0.2472
5% Ni	250	−0.14 ± 0.05	0.62 ± 0.11	18.7 ± 0.3	1.40×10^6	0.1029
10% Re	250	−0.09 ± 0.05	0.55 ± 0.11	17.9 ± 1.6	2.58×10^6	0.3839
10% Cu	130	0.30 ± 0.05	0.38 ± 0.19	13.3 ± 0.8	1.44×10^6	12.1900
5% Au	270	0.74 ± 0.02	0.13 ± 0.10	11.6 ± 0.6	9.46×10^2	0.0356

[a] Temperature at which reaction orders were determined, °C.
[b] Order with respect to CO.
[c] Order with respect to H_2O.
[d] Apparent activation energy, kcal/mole.
[e] Preexponential factor, molecules/sec/metal site, in the equation $N = A \exp(-E/RT)$.
[f] Turnover number at 1 hr on stream and conditions of 300°C, $P_{CO} = 24.3$ kPa, $P_{H_2O} = 31.4$ kPa.
[g] The activity of the metal-free Al_2O_3 support is one-tenth that of the least active metal, Ir.

respect to water and carbon monoxide are included in Tables 2 and 3. For water the order of reaction varies from near zero to about 0.8. For carbon monoxide, the reaction order varies from about −0.4 to approximately +0.6 order.

The effect on activity of changing support for Pt and Rh is presented in Table 3. It is clear that the support has a major effect on the activity. Pt/SiO_2 has only $\frac{1}{10}$th the specific activity of Pt/Al_2O_3. Pt/C is even less active with a specific activity nearly two orders of magnitude lower than Pt/Al_2O_3. This support effect is not unique to Pt since Rh/SiO_2 has about $\frac{1}{13}$th the activity of Rh/Al_2O_3 as shown in Table 3. As discussed below, a similar large support effect has been observed previously for the TSD reaction (*3*).

Because H_2O is a potential oxidant, the possibility exists that some of the metals may become oxidized during reaction. While it is difficult to detect or even predict surface oxidation of small metal crystallites, it is possible to use bulk thermodynamic properties to assess the driving force for oxidation. Of the metals studied, only the first period metals and perhaps Re would be suspected of potential oxidation under reaction conditions. Consider the following reactions and their values for the reaction free energy of formation, ΔF_r, at 600°K (327°C):

$$Fe + H_2O \rightarrow FeO + H_2 \qquad \Delta F_r = -2.65 \text{ kcal/mole},$$

$$Co + H_2O \rightarrow CoO + H_2 \qquad \Delta F_r = +4.50 \text{ kcal/mole},$$

$$Ni + H_2O \rightarrow NiO + H_2 \qquad \Delta F_r = +6.90 \text{ kcal/mole},$$

$$2Cu + H_2O \rightarrow Cu_2O + H_2 \qquad \Delta F_r = +20.65 \text{ kcal/mole},$$

$$Re + 3H_2O \rightarrow ReO_3 + 3H_2 \qquad \Delta F_r = +44.45 \text{ kcal/mole}.$$

From the above results it is seen that only Fe has an appreciable tendency toward bulk oxidation in the presence of water. It is interesting to note that the orders of

TABLE 3

A Comparison of the Kinetic Parameters of Alumina- and Nonalumina-Supported Metals

Catalyst	T^a	^{b}	^{c}	E^d	A^e	N^f	Relative activity
Pt/Al_2O_3	270	−0.21 ± 0.03	0.75 ± 0.04	19.6 ± 1.3	1.90×10^6	0.0635	90
Pt/SiO_2	340	−0.08 ± 0.05	0.69 ± 0.08	19.1 ± 0.8	1.18×10^5	0.0061	9
Pt/C	340	0.13 ± 0.05	0.35 ± 0.17	25.5 ± 1.4	3.84×10^6	0.0007	1
Rh/Al_2O_3	330	−0.10 ± 0.02	0.44 ± 0.02	23.0 ± 1.3	5.10×10^6	0.0086	13
Rh/SiO_2	350	−0.24 ± 0.03	0.53 ± 0.12	22.8 ± 2.5	3.23×10^5	0.0007	1

[a] Temperature at which reaction orders were determined, °C.
[b] Order with respect to CO.
[c] Order with respect to H_2O.
[d] Apparent activation energy, kcal/mole.
[e] Pre-exponential factor, molecules/sec/metal site in the equation $N = A \exp(-E/RT)$.
[f] Turnover rate after 1 hr on stream and conditions of 300°C, P_{CO} = 24.3 kPa, P_{H_2O} = 31.4 kPa.

reaction for CO and H_2O over the Fe catalyst are markedly different from all the other Group VIII metals. For Fe the CO order is about 0.6 whereas the other metals have CO orders of reaction near zero. Also the water order of reaction for Fe is about zero while the other Group VIII metals are about ½. These differences suggest that the Fe catalyst surface may be partially oxidized under reaction conditions.

DISCUSSION

This section is divided into three segments. First, the periodic trends of the activities of the various metals studied will be presented. Next the effect of support on the activities of the metals will be discussed. Finally, a reaction sequence incorporating both metal function and support function will be given.

Periodic Table Trends

In heterogeneous catalysis, it is useful to observe the periodic trends of kinetic parameters such as activation energies, activities, and selectivities. In this manner the trends observed among a series of catalysts prepared from neighboring metals of the periodic table may in turn be correlated with other physical properties of the catalysts under study. For example, Sinfelt (*13*) has shown that a metal's activity for ethane hydrogenolysis bears the same general periodic trends as does the metal's percentage *d*-character. A plot of turnover rate of the alumina-supported metals for WGS as a function of their periodic table position is given in Fig. 1. For the Group VIII noble metals there is a minimum in activity at the Group $VIII_2$ metals, Rh and Ir. Among these six noble metals the WGS activity does not vary drastically, in contrast to the ethane hydrogenolysis reaction (*13*). The

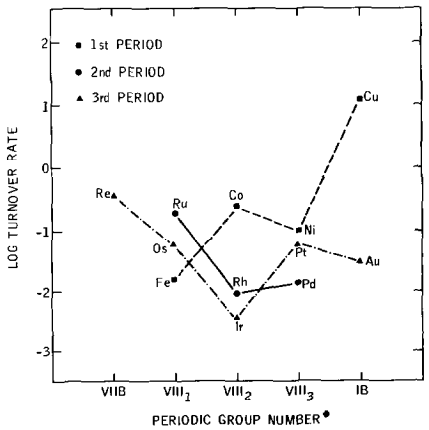

FIG. 1. Periodic trends of the activity of alumina-supported metals for the WGS reaction. Activities are turnover rates at 300°C and partial pressures of H_2O and CO of 31.4 and 24.3 kPa, respectively.

least active metal, Ir, is only 60 times less active than the most active noble metal, Ru. This contrasts sharply with the nearly seven orders of magnitude range of specific activities (*13*) for ethane hydrogenolysis over these same six metals. Clearly the WGS reaction is much less sensitive to the structural and electronic property variations of these metals when compared to the ethane hydrogenolysis reaction.

Because of the increasing interest in CO chemistry over transition metals, the studies of the WGS reaction were extended to include selected nonnoble metal catalyst systems. The activities of these additional metals are compared to the noble metal activities in Fig. 1. The periodic trends observed for the iron triad metals (Fe, Co, Ni) are opposite to those observed for the noble metals. The Group $VIII_2$ metal, Co, is the most active in the first period whereas Rh and Ir are the least active of the noble metals. Nevertheless the Group VIII metals demonstrate a relatively nonspecific response to the WGS reaction in the sense that the activities of all the Group VIII metals are within two orders of magnitude of each other.

As mentioned in the Introduction the high-activity, low-temperature water gas shift catalyst is based on copper metal. The high activity of Cu relative to the other metals studied is evident from Fig. 1. Cu is 50 times more active than the most active Group VIII metal, Co, and is almost 4000 times more active than the least active of the Group VIII metals, Ir.

Frequent uses of correlations between kinetic parameters and the physical properties of catalysts or, more desirably, the physical properties of intermediates on the surface have been attempted. One such correlation is based on Sabatier's principle (*14*) which states that the properties of surface intermediates may qualitatively resemble the properties of bulk compounds that are available for study. An example of this would be the decomposition of formic acid over metal catalysts. For this reaction it is possible to correlate the rate of formic acid decomposition on a metal with the corresponding heat of formation of the bulk metal formate compound (*14*). It would, of course, be more desirable to correlate catalyst activity with a property of an actual surface intermediate (ideally the most stable one) which occurs in the catalyzed chemical reaction.

Accordingly, for the WGS reaction it would be reasonable to expect a relationship between the activity of the metal catalyst and the strength of interaction of CO with the metal. Using the heats of adsorption data for CO on various metals as tabulated by Vannice (*15*), a correlation between the heat of adsorption of CO and the metal's activity can be constructed (Fig. 2). The heats of adsorption used in Fig. 2 are for pure metals (see Ref. (*15*). Thus, the assumption is made that these heats of adsorption for the pure metals are similar to the heats of adsorption of the metals supported on alumina. This is a reasonable assumption for a support such as Al_2O_3 but may not be for other supports such as TiO_2 (see Ref. (*16*)). Of the noble metals for which data are available, the CO heats of adsorption vary from about 29

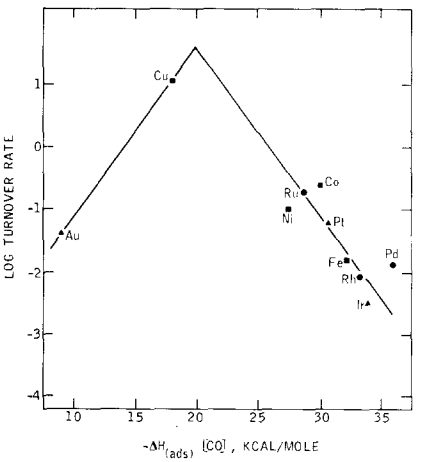

FIG. 2. Volcano-shaped relationship between metal turnover number at 300°C and heat of adsorption of carbon monoxide.

kcal/mole for Ru to 36 kcal/mole for Pd, a range of only 7 kcal/mole. Correspondingly, the activities of these metals vary by a relatively small factor of 60. It appears that the narrow range of activities among the noble metals is related to the narrow range of strengths of CO interaction with the metals.

In addition to the noble metals, Fig. 2 also includes the remaining metals that have been studied for which CO heats of adsorption data are available. The addition of Cu and Au catalysts to the correlation of activity with CO heat of adsorption appears to complete the left-hand side of a typical volcano-shaped plot. This type of correlation is in accordance with Sabatier's principle (*14*). Because we assume the intermediate CO–M is involved in the surface chemistry (see Reaction Sequence section), one would expect the observed correlation between catalyst activity and stability of the CO–M intermediate (CO–M represents chemisorbed CO). For metals that chemisorb CO weakly such as Au, the activity will be low because the corresponding concentration of CO–M species will be low. The weak interaction of CO with Au is consistent with the observed high CO order of reaction for Au relative to most of the other metals (see Table 2). On the other hand, if the CO–metal interaction is very strong, then the CO–M intermediate becomes so stable that subsequent reaction to product becomes low. This appears to be the case for some of the noble metals such as Pd and Ir (see Fig. 2). The near-zero order of reaction for many of these metals is consistent with a much stronger interaction of CO with the metals.

For a surface intermediate such as CO–M there should be an optimum strength of interaction between adsorbent and adsorbate so that the interaction is strong enough to provide a sufficient concentration of the intermediate species but not strong enough to prevent subsequent reaction of the intermediate to products. For the WGS reaction, as shown in Fig. 2, this optimum strength of interaction of CO and metal appears to be near 20 kcal/mole. It is interesting to note that Vannice (*15*) reported a similar volcano-shaped relationship between the heat of adsorption of CO and the metal's activity for CO methanation ($CO + 3H_2 \rightarrow CH_4 + H_2O$). Vannice, however, found that the optimum metal–CO interaction for maximum methanation activity was about 30 kcal/mole which suggests that a stronger interaction of CO with the metal is necessary for CO reduction.

Support Effects

One motivation of this water gas shift study over supported noble metals was to compare the effect of changing supports on activity for WGS and toluene steam dealkylation. Support effects on the TSD reaction (Eq. (5)) were previously discussed (*3*). It was shown that Rh/Al_2O_3 is 37 times more active than Rh/SiO_2, 70 times more active than Rh/C, and 200 times more active than an unsupported Rh black catalyst. The results presented in Table 3 for the WGS reaction show similarly large effects on the metal's activity. For both Rh and Pt, with each highly dispersed on all supports, there are still order of magnitude effects on specific activity. The effect of support for both WGS and TSD is thus comparable, with Al_2O_3-supported catalysts being the most active. Silica-supported metals have lower activity and metals supported on nonoxides such as carbon still lower activity.

In order to define the large support effects observed in the TSD reaction, a similar reaction, the toluene hydrodealkylation reaction (THD), was also investigated over a series of supported catalysts. The effect of changing support on the activity of Rh for the following two reactions was investigated:

$$\text{TSD: } \phi\text{-}CH_3 + H_2O \rightarrow \phi\text{-}H + CO + 2H_2, \quad (6)$$

$$\text{THD: } \phi\text{-}CH_3 + H_2 \rightarrow \phi\text{-}H + CH_4. \quad (7)$$

It was found that the activity of Rh for the THD reaction was virtually independent of support (*3*). This behavior reinforced our conclusion that the strong support effect in the TSD reaction is due to support sites necessary for water activation.

A similar comparison is made for the WGS reaction by comparing the effect of changing support on the WGS and methanation reactions:

$$\text{WGS: } CO + H_2O \rightarrow CO_2 + H_2, \quad (8)$$

$$\text{SGR: } CO + 3H_2 \rightarrow CH_4 + H_2O. \quad (9)$$

Vannice (*17*) has studied the kinetics of reaction (9) over Al_2O_3-supported metals. He recently presented similar activity results (see Ref. (*15*)) for SiO_2-supported metals. From these two sets of data for the SGR reaction, Pt/Al_2O_3 is found to be only 1.7 times more active than Pt/SiO_2 and Rh/Al_2O_3 is about 1.7 times more active than Rh/SiO_2. The WGS activities of these pairs of catalysts differ by about an order of magnitude as discussed above. As with the TSD/THD reaction couple, the support has a much stronger effect toward reactions requiring activation of H_2O, supporting the notion that water is principally activated on support sites. We conclude that both TSD and WGS reactions occur bifunctionally in the sense that the metal activates hydrocarbon or carbon monoxide whereas support sites are the principal sites for water activation.

With bifunctional reactions over supported metal catlysts, the question arises as to whether the metal–support interface is the active center. One means of addressing this for supported metals is to vary the dispersion of the metal component and then compare the turnover rates for the catalysts. If the active sites are restricted to the metal–support interface, then one would anticipate that poorly dispersed catalysts would have lower turnover rates since there is a smaller fraction of the available metal sites in contact with the support. Table 4 shows the effect of dispersion on turnover rate for the WGS reaction. The turnover rate is essentially constant over a wide range of metal dispersions. We therefore conclude that the active metal sites consist of all the exposed metal surface area rather than only the metal sites in direct contact with the surface. The results in Table 4 are also strong evidence for the WGS reaction being a facile or structure-insensitive reaction.

TABLE 4

Effect of Metal Dispersion on Specific Activity of Rhodium for the WGS Reaction

Catalyst	Fraction metal exposed	Turnover rate at 300°C (molecules/sec/site)
1% Rh/Al_2O_3	1.0	0.0086
5% Rh/Al_2O_3	0.29	0.0073
5% Rh/Al_2O_3	0.18	0.0093

Reaction Sequence

To be consistent with the experimental observations noted above, a reaction sequence will have to account for both the role of the metal and the role of the support. If the support is the source for water activation, we can write the following for water activation on support sites:

$$H_2O + S\text{–}O\text{–}S \overset{K_1}{\longleftrightarrow} 2\ OH\text{–}S, \quad (10)$$

$$H_2O + S \overset{K_2}{\longleftrightarrow} H_2O\text{–}S. \quad (11)$$

Reaction (10) is the dissociative adsorption of H_2O onto support sites. For example, with Al_2O_3 reaction (10) can be written as

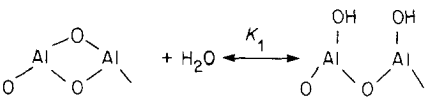

(12)

The nondissociative adsorption of water (reaction (11)) on Al_2O_3 can be written as

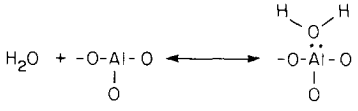

(13)

where the water is chemisorbed at the Lewis acid centers of Al_2O_3. It is probable that under reaction conditions both types of water adsorption are taking place. Since the reaction temperatures employed for WGS are in the range where Al_2O_3 typically begins to undergo dehydration, the concentration of adsorbed water, particularly of the nondissociated form, should be low since higher temperatures are typically needed to dehydroxylate Al_2O_3.

We may propose formic acid as an intermediate since the two principal decomposition pathways for formic acid involve both the reactants and the products of the WGS reaction as follows:

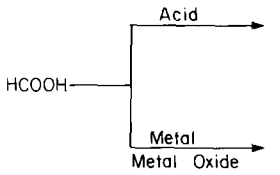

$$CO + H_2O \quad (14)$$

$$CO_2 + H_2 \quad (15)$$

The decomposition of formic acid, particularly over oxides, has been widely studied. Both Krylov (*18*) and Trillo *et al.* (*19*) review the decomposition reaction over metal oxides, and Bond (*20*) summarized the conversion reaction over metals. Reaction (14), the dehydration reaction, is catalyzed by acid oxides such as Al_2O_3. Reaction (15), the dehydrogenation reaction, on the other hand, is more readily catalyzed by metals and basic metal oxides (*19, 20*).

Amenomiya (*21, 22*) has recently discussed the kinetics of the forward and reverse WGS reactions over Al_2O_3. Using infrared spectroscopy, Amenomiya (*22*) was able to identify the presence of formate ions in both the forward and the reverse WGS reactions. He thus concluded that the formate ion was an intermediate in the WGS reaction. Therefore, depending on the direction of the WGS reaction, formate ion is decomposed into either CO_2 and H_2 or CO and H_2O. In either case, a proton from the alumina is necessary to satisfy stoichiometry. Noto *et al.* (*23*) have studied the decomposition of formic acid over alumina. Here, because of the acidic nature of the alumina, the decomposition proceeds via dehydration to CO and H_2O. These authors also observed formate ions, but concluded that the formate ions were not intermediates in the decomposition reaction. Instead they maintained that the adsorbed proton from the dissociative adsorption of formic acid to form formate ion and adsorbed hydrogen was the active site for decomposition. There appears to be little doubt that formate ions and thus presumably formic acid may be present during the WGS reaction. The exact nature of the intermediate species remains in doubt, however. The following analysis thus assumes the stoichiometric presence of formic acid although the work of Amenomiya suggests that labile protons are available to allow for formate ion decomposition.

In order to account for the large activity increase due to the presence of metal sites as compared to pure alumina, one assumes that CO is more effectively provided from adjacent metal sites than Krylov's (*24*) direct activation from the gas phase. We can write the formation of formic acid via the reverse of reaction (14) over Al_2O_3 as follows:

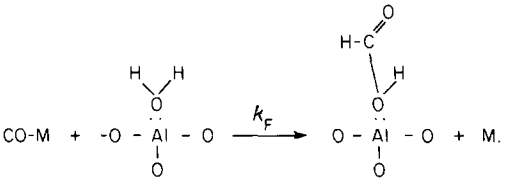

(16)

In reaction (16), CO–M represents the concentration of carbon monoxide chemisorbed on the metal surface. For simplicity we will refer to the H_2O–surface complex as W–S and the formic acid–surface complex as F–S. The concentration of F–S is taken to be proportional to the product of the concentration of CO on metal sites, (CO–M), and the concentration of nondissociated H_2O chemisorbed on support sites, (W–S). Assuming Langmuir adsorp-

tion isotherms for CO on metal sites and H_2O on support sites, the fractional coverage of formic acid on support sites would be given by

$$\Theta_{(F-S)} = k_F \Theta_{(CO-M)} \Theta_{(W-S)}.$$

If $\Theta_{(F-S)}$ is small, the concentration of undissociated water on support sites is

$$\Theta_{(W-S)} = \frac{K_2 P_W}{[1 + K_2 P_W + (K_1 P_W)^{1/2}]}, \quad (17)$$

where K_1 and K_2 are equilibrium adsorption constants for water according to reactions (10) and (11) given above. If K_1 and K_2 are small or the partial pressure of water is small, $\Theta_{(F-S)}$ can be simplified to

$$\Theta_{(F-S)} = k' \Theta_{(CO-M)} P_W. \quad (18)$$

On metal sites the formic acid species, F–S, can dehydrogenate according to reaction (15). We can write this decomposition reaction as follows:

$$F\text{–}S + M \xrightarrow{k_{WGS}} F\text{–}M + S \quad (19a)$$

$$F - M \xrightarrow{\text{fast}} CO_2 + H_2 + M, \quad (19b)$$

where M represents a vacant metal site.

Reaction (19) represents the transport and adsorption of the formic acid intermediate from the support to a bare metal site followed then by the rapid decomposition of the metal–formic acid species into the products, CO_2 and H_2. This reaction is reasonable if we consider two points. If the subsequent metal-catalyzed formic acid decomposition is rate limiting, then the activities of the metals for WGS should correlate with the activities of the metals for formic acid decomposition. If one compares the rank order of metal activity of formic acid decomposition using data reported by Bond (*25*) with the corresponding rank order of metal activity for WGS, the resulting plot shows no correlation (rank order correlation constant = −0.18). This indicates no relationship between the activities of metals for formic acid decomposition and the activities of the same metals for WGS. More recently, Madix (*26*) studied the decomposition of formic acid on clean metal surfaces. He reported that the decomposition reaction on Ni takes place at temperatures as low as 100°C, a temperature much below the typical reaction temperatures used for the WGS reaction. We thus conclude that the decomposition of the formic acid–metal complex is rapid relative to its formation on the metal surface by migration from the support. Also it is evident that the transport to and the adsorption of formic acid onto the metal are essentially irreversible due to its rapid decomposition.

According to reaction (19), the rate of the WGS reaction is

$$r_{WGS} = k_{WGS}\, \Theta_{(F-S)}\, (\Theta_M), \quad (20)$$

where Θ_M represents the fraction of unoccupied metal sites. Both CO and H_2O will compete strongly with the easily decomposed intermediate, (F–S), for metal sites. If we assume the adsorption of CO onto metal sites to be nondissociative, we can write

$$CO + M \xleftrightarrow{K_{CO}} CO\text{–}M. \quad (21)$$

If we assume the adsorption of water on metal sites to be dissociative we can write

$$H_2O + 2M \xleftrightarrow{K_W} OH\text{–}M + H\text{–}M. \quad (22)$$

Assuming Langmuir adsorption isotherms for CO and H_2O adsorption on metal sites, the fraction of unoccupied metal sites, Θ_M, is given by

$$\Theta_M = \frac{1}{[1 + K_{CO} P_{CO} + (K_W P_W)^{1/2}]}. \quad (23)$$

The rate of the WGS reaction (formation of CO_2 and H_2) is obtained by substituting into Eq. (20) values for (Θ_{F-S}) from Eq. (18) and for Θ_M from Eq. (23). Thus the WGS rate is

$$r_{WGS} = k_{WGS}\, K'\, \Theta_{CO-M} P_W \left\{ \frac{1}{1 + K_{CO} P_{CO} + (K_W P_W)^{1/2}} \right\}. \quad (24)$$

The fraction of metal sites covered by CO, Θ_{CO-M}, is given by the expression

$$\Theta_{CO-M} = \frac{K_{CO}P_{CO}}{[1 + K_{CO}P_{CO} + (K_WP_W)^{1/2}]}. \quad (25)$$

Substituting this into Eq. (24) gives

$$r_{WGS} = k_{WGS}\, k'\, K_{CO}P_{CO}P_W \left\{\frac{1}{1 + K_{CO}P_{CO} + (K_WP_W)^{1/2}}\right\}^2. \quad (26)$$

If $K_{CO}P_{CO} + (K_WP_W)^{1/2} \gg 1$ as is consistent with our binding assumptions for these species, then Eq. (26) can be rearranged to

$$r_{WGS} = k''\, K_{CO}P_{CO} \left\{\frac{[(K_WP_W)^{1/2}/K_{CO}P_{CO}]}{1 + (K_WP_W)^{1/2}/K_{CO}P_{CO}}\right\}^2. \quad (27)$$

Equation (27) can be further simplified by the use of the well-known approximation of the term $ax/(1 + ax)$ by the term bx^n, where b and n are constants with n constrained to the range $0 < n < 1$. Thus Eq. (27) becomes

$$r = k'b\, K_{CO}P_{CO} \left\{\frac{(K_WP_W)^{1/2}}{K_{CO}P_{CO}}\right\}^{2n} \quad (28)$$

which provides a power rate law expression of the WGS rate:

$$r = k\, P_{CO}^X P_W^Y = k\, P_{CO}^{1-2n} P_W^n. \quad (29)$$

For convenience this expression may be rearranged to give

$$r = k\, P_{CO}^X P_W^{(1-X)/2}. \quad (30)$$

For this rate expression to be valid, the experimental water order of reaction, Y(expt), must be in the range $0 < Y(\text{expt}) < 1$ which is the case as shown in Table 2. Equation (29) predicts an opposing relationship between the CO and the H_2O orders of reaction. Experimentally, this relationship is observed as shown in Fig. 3. To test the validity of Eq. (30), we can use the form of Eq. (30) to calculate the water order of reaction, Y(calc), given the experimental CO order of reaction, X(expt). Thus, Y(calc) is given by the expression [1 − X(expt)]/2, where X(expt) is the observed experimental CO order of reaction. If this calculation is carried out for each metal, Fig. 4 can be constructed where the calculated water reaction order is compared to the experimental water reaction order. The agreement between calculated and experimental water reaction orders is good for all metals studied. Thus the approach of assuming a formic acid intermediate participating in a bifunctional surface sequence leads to a simple power rate law expression for the WGS reaction which is consistent with the experimental reaction orders for a wide variety of alumina-supported metals.

This bifunctional approach helps to explain other features presented in this paper. The effect of support on the WGS rate may be related to the acidity of the various oxide supports. Since SiO_2 has much less Lewis

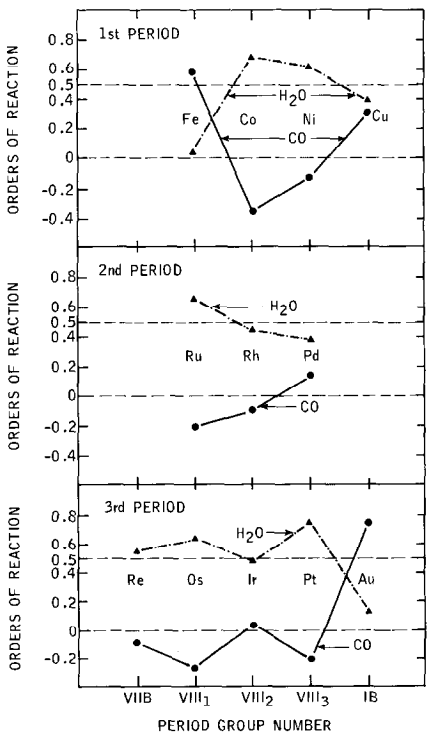

FIG. 3. Periodic trends of H_2O and CO orders of reaction for alumina-supported metals. The reaction orders were determined at the temperatures listed in Table 2.

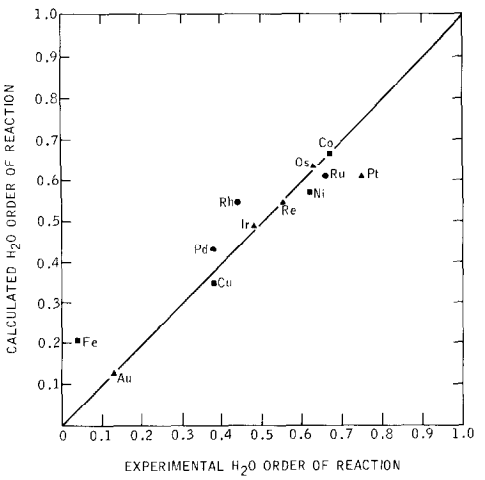

FIG. 4. Comparison of calculated H_2O orders of reaction with experimentally determined H_2O orders of reaction. The calculated H_2O values are from the expression $(1 - X)/2$, where X is the experimentally determined CO order of reaction.

acidity than Al_2O_3, it is reasonable that the concentration of the formic acid intermediate (F–S) on such sites would be much lower on SiO_2 than on Al_2O_3. According to reaction (20) this would lead to a reduced bifunctional rate of reaction on SiO_2 compared to Al_2O_3, in agreement with the rate data shown in Table 3. If only the concentration of the formic acid intermediate changes upon changing from Al_2O_3 to SiO_2, the activation energy should not change if the metals behave similarly on both supports. As shown in Table 3, the activation energies of Pt supported on Al_2O_3 and SiO_2 are similar as are the activation energies for Rh supported on Al_2O_3 and SiO_2. The change in activation energy for Pt/C compared to Pt supported on the two oxides suggests a more complex situation. For Pt/C there may be so few sites available for H_2O activation that H_2O activation becomes rate limiting.

The above analysis also helps explain the correlation between the CO heat of adsorption onto the metals and the WGS rate of reaction as shown in Fig. 2. The equilibrium concentration of CO adsorbed on metal sites, $\Theta_{(CO-M)}$, should increase monotonically with the strength of the metal–CO interaction. Equation (18) indicates that $\Theta_{(F-S)}$, the concentration of the formic acid intermediate, will behave similarly. However, the fraction of unoccupied metal sites will decrease with increasing strength of the metal–CO interaction. The form of Eq. (20) thus indicates that there has to be an optimum balance in the respective concentrations for maximum WGS activity. From Fig. 2, the optimum CO–metal strength of interaction appears to be about 20 kcal/mole, which is near the heat of adsorption of CO on Cu metal. For metals with stronger CO heats of adsorption, the right side of the volcano-shaped correlation, the concentration of vacant metal sites, Θ_M, may be the limiting factor for WGS activity. With Au which has a very low CO heat of adsorption, the limiting factor may become the surface concentration of CO, Θ_{CO-M}.

Alternatively, the volcano relationship can be explained by considering that the rate of CO transport from the metal to the support would be proportional to the inverse of the strength of the CO–metal interaction and directly proportional to the concentration of CO on the metal surface. Again there would be an optimum metal–CO interaction where the CO concentration is high enough and the metal–CO interaction weak enough to allow for an optimum rate of transport of CO to support sites. Additional studies will be necessary to discern which combination of the above factors best explains the observed effect of CO–metal interaction on WGS activity.

Recently, attention has been focused on homogeneous catalysts for the WGS reaction (*27*). Interestingly, many of the active homogeneous WGS systems employing a basic medium are thought to involve a formate intermediate in the reaction sequence (*4*). As shown above, the use of a formic acid intermediate in the heterogeneous reaction sequence also accounts for the observed kinetics over a wide variety of metal catalysts.

The reaction sequence discussed above shows much promise for explaining the kinetics of the WGS reaction over a wide variety of metals and metal–support combinations. One must be cautious, however, because of the large number of assumptions necessary in such a kinetic analysis. For example, there are the well-known limitations of using Langmuir adsorption isotherms. Nevertheless, the kinetic analysis still leads to a rate expression consistent with the experimental results as well as provides for reasonable explanations of both metal and support effects. Most importantly, however, the proposed reaction sequence helps explain the complex interrelationship of metal and support functions in the CO/H_2O reaction system.

REFERENCES

1. Thomas, C. L., "Catalytic Processes and Proven Catalysts." Academic Press, New York, 1970.
2. Grenoble, D. C., *J. Catal.* **51,** 203 (1978).
3. Grenoble, D. C., *J. Catal.* **51,** 212 (1978).
4. Laine, R. M., Rinker, R. G., and Ford, P. C., *J. Amer. Chem. Soc.* **99,** 252 (1977).
5. Rostrup-Nielsen, J. R., "Steam Reforming Catalysts." Teknisk Forlag A/S, Copenhagen, 1975.
6. "Catalyst Handbook," Imperial Chemical Industries Ltd. Wolfe, London, 1970.
7. Prichard, C. R., and Hinshelwood, N., *J. Chem. Soc.* **127,** 806 (1925).
8. Masuda, M., and Migahrua, K., *Bull. Chem. Soc. Japan* **47,** 1058 (1974).
9. Masuda, M., *J. Res. Inst. Catal. Hokkaido Univ.* **24,** 83 (1976).
10. Shelef, M., and Gandhi, H. S., *Ind. Eng. Chem. Prod. Res. Develop.* **13,** 80 (1974).
11. Taylor, K. C., Sinkevitch, R. M., and Klimisch, R. L., *J. Catal.* **35,** 34 (1974).
12. Grenoble, D. C., *J. Catal.* **56,** 32 (1979).
13. Sinfelt, J. H., *Catal. Rev.* **3,** 175 (1969).
14. Discussions of Sabatier's principle can be found in the following: Boudart, M., "Kinetics of Chemical Processes," p. 198. Prentice–Hall, Englewood Cliffs, N.J., 1968. Gates, B. C., Katzer, J. R., and Schuit, G. C. A., "Chemistry of Catalytic Processes," p. 206. McGraw-Hill, New York, 1979.
15. Vannice, M. A., *J. Catal.* **50,** 228 (1977).
16. Tauster, S. J., Fung, S. C., and Garten, R. L., *J. Amer. Chem. Soc.* **100,** 170 (1978).
17. Vannice, M. A., *J. Catal.* **37,** 449 (1975).
18. Krylov, O. V., "Catalysis by Non-Metals," p. 134. Academic Press, New York, 1970.
19. Trillo, L. M., Munuera, G., and Criado, J. M., *Catal. Rev.* **7,** 51 (1972).
20. Bond, G. C., "Catalysis by Metals," p. 412. Academic Press, New York/London, 1962.
21. Amenomiya, Y., *J. Catal.* **55,** 205 (1978).
22. Amenomiya, Y., *J. Catal.* **57,** 64 (1979).
23. Noto, Y., Fukida, K., Onishi, T., and Tamaru, K., *Trans. Faraday Soc.* **63,** 2300 (1967).
24. Krylov, O. V., "Catalysis by Non-Metals," p. 137. Academic Press, New York, 1970.
25. Bond, G. L., "Catalysis by Metals," p. 430. Academic Press, New York/London, 1962.
26. Madix, R. J., *Catal. Rev.* **15,** 293 (1977).
27. *C & E News* **55,** 17 (1977).